



Modeling and evaluating mixing streams for an innovative design of a stationary elements' mixer

Khalid Abdulsada Mter¹, Ali Mohammad Ali¹, Khairi R. Kalash¹,
Hayder Abdulkhaleq Alalwan^{2*} , Malik Mustafa Mohammed³ ,
Ahmed Q. Mohammad⁴, Fatima Shuwaikh⁵

¹ Scientific Research Commission, Baghdad, Iraq

² Fuel and Energy Techniques Department, Technical Engineering College- Baghdad, Middle Technical University, Baghdad, Iraq

³ University of Warith Al-Anbiyaa, Karbala, Iraq

⁴ College of Engineering, Al-Naji University, Baghdad, Iraq

⁵ Gulf University, Sanad, 26489, Kingdom of Bahrain

* Corresponding author's e-mail: hayder.alalwan@mtu.edu.iq

ABSTRACT

The trade-off between mixing efficiency, energy consumption, and low maintenance costs presents a compelling reason to further explore energy-free and environmentally friendly hydraulic mixing. This research focused on designing a low-complexity static mixer with fixed components that achieves high efficiency while minimizing pressure drop and kinetic energy usage. The innovative mixer developed in this study adopted Tesla's micromixer structure, featuring a diameter of 170 mm and a height of 600 mm, making it an appropriate size for water treatment applications. To validate the effectiveness of this size Tesla-style mixer, computational fluid dynamics (CFD) were utilized to model the mixing currents created by vortices. The results indicated a promising mixing efficiency between coagulants and contaminants. Additionally, the study examined two optimized designs for the innovative mixer: one with sharp edges for the internal channels and another with rounded edges. To ensure accuracy in the analysis, the Realizable K- ϵ model was selected, known for its effectiveness in simulating high-intensity disturbances and complex flow conditions similar to those in this study. The sharp-edged design showed superior performance. Encouraging additional adjustments by increasing the number of mixing stages for the same size of the mixer. These enhancements improved mixing efficiency, as indicated by the pressure drop parameters and mixing VOF ratios for water and coagulants.

Keywords: mixing efficiency, energy consumption, static mixer, Tesla's micromixer structure, coagulants; mixing stages.

INTRODUCTION

Water and wastewater treatment have attracted high attention due to the vital roles of water in different aspects [1, 2]. Different treatment processes have been investigated, with a focus on novel solutions such as using nanoparticles due to their high surface area [3], reactivity [4], adsorption capacity [5], and other unique advantages [6–8]. The mixing process is a vital step in water treatment systems, as it requires the rapid diffusion of coagulants in raw water

to interact with various pollutants, forming coagulant flocks with the densities that allow the deposition of these contaminants [9–11]. The importance of using stationary mixers in multiple industries has increased over the past few years, including the water treatment sector [12, 13]. These mixers do not have moving parts, resulting in lower maintenance, operating costs, and space requirements. Stationary mixers can work with different liquids and gases, from low viscosity to highly viscous non-Newtonian liquids [14, 15].

A stationary mixer is designed to overcome several frequent or disparate obstacles within a pipe or channel to excite the mixing of flowing fluid streams.

Ramin Rahmani et al. examined the performance of the helical stationary mixer has been analyzed under turbulent flow conditions using numerical simulations. The model employs the three-dimensional Reynolds–Navier–Stokes equations with the Sballart–Almaras turbulence model and a second-order accurate finite-volume method. Simulations of the six-element mixer assess mixing results and stationary mixer performance with various predictive tools [16, 17].

Banerjee, A. et al. analyzed turbulent flow in 90° mixing elbows, rather than on helical static mixers using the k-epsilon model. They examined the Reynolds numbers and mixing efficiency through the fluid behavior on the bending curvature [18].

The performance of the static mixer is practically evaluated by measuring the mixing efficiency and pressure drop. For this purpose, the pressure drop is defined as the Z-ratio of pressure drop (the pressure drop in the mixer to the pressure drop that occurs in a normal pipe) [19]. On the basis of physical principles, the optimal static mixer is the one that achieves a high degree of mixing while minimizing pressure drop. This is achieved by converting the momentum of the liquids into mechanical energy for static mixing, which can result in lesser pressure drop [20, 21].

Although mixing elements in static mixers are intended to mix liquids, they can somehow hinder flow streams [22]. The complexities of combining elements in stationary mixers can increase the pressure drop and thus reduce mixing efficiency. To improve mixing efficiency, the methods to minimize flow obstruction while maintaining a constant flow momentum and a low difference between the pressure at the inlet and outlet of the mixer need to be found [23].

The main objective of this research was to conduct a numerical analysis to create a static mixer with fewer numbers and simpler geometric shapes for fixed internal mixing elements that achieve optimal mixing of streams of contaminated coagulants and water with high mixing efficiency while maintaining an acceptable level of flow pressure inside the mixer [24]. This can lead to significant energy savings.

To improve mixing efficiency, innovative solutions should focus on reducing the number of

mixing elements that usually slow down the flow while maintaining the appropriate pressure drop to increase mixing efficiency and maintain cohesive momentum in the mixing [25]. One way to maintain flow momentum is by increasing the kinetic energy required to self-drive the flow, which can be achieved by modifying the internal geometry of the mixing device without relying on the concept of obstruction of flow [26]. To achieve a sufficient momentum for the continuous flow of liquids towards the mixing paths and counteract the pressure drop that usually occurs in stationary mixers, it is possible to imitate the well-known flow behavior in Tesla valves [27].

Nikola Tesla created the Tesla valve in 1920 [28]. A Tesla valve is a type of fluid guide valve that controls the flow of liquids or gases in a particular system. Its basic design consists of a series of channels or small chambers to drive the flow in one direction. The valve structure consists of a connected main channel and a series of interconnected curved sub-channels opened to the main channel with repeated symmetrical distances that allow the liquid to flow in one direction, see Figure 1.

A liquid or gas can pass through the main channel with very little opposition (high flow direction) [29]. If a liquid or gas flows in the opposite direction (low flow direction), the flow branches towards the main channel and the curved sub-channels, and then vortex reverse flows form at all the areas where those curved sub-channels meet the main channel. This increases the amount of energy and momentum required to push the liquid or gas in this direction [30].

Hong et al. [31] developed a micromixer that exploits the “Coanda effect” that produces cross-wise branching with modified Tesla structures. Part of the flow is directed from a separate inlet around a curved channel to create the mixing streams that oppose the flow in the main channel. Naturally, the flow wants to move to the side channels, which then rotate and push back into the main channel, causing eddies in the area of its confluence with the main channel. These vortices increase the energy needed to push the flow lines towards the low flow of the Tesla valve, compensating for the natural drop of pressure that occurs inside the mixer.

Wang et al. created a liquid-liquid extractor using a feedback liquid oscillator. The design was formed based on the Coanda effect, as the designed oscillator was linked to two feedback channels to ensure thorough mixing of the aqueous and

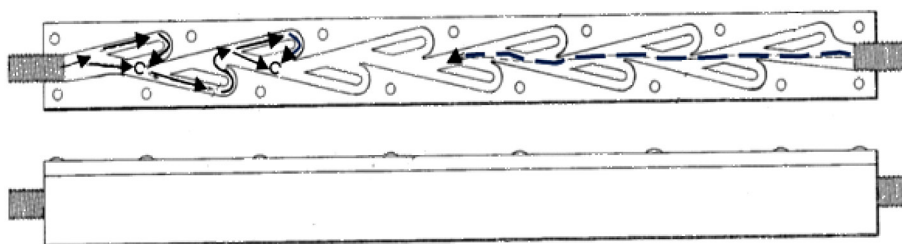


Figure 1. Tesla valve conduit [28]

organic phases. During visual observation, it was noticed that the aqueous phase was dispersed in small droplets due to liquid oscillation and vortex formation caused by the confluence of flows from the end of the two channels with the flow in the main space of the oscillator [32].

This paper presents an innovative design of a relatively large-volume stationary mixer that uses minimal structural engineering complexity for testing. The mixer was designed to overcome the issue of common pressure drop in stationary mixers. The design integrated the principles of Tesla valve flow and the Coanda effect. The flow of two different liquids was passed through branched passages, and when they met in the main passage, they created vortices that increased the flow momentum towards the mixing streams. This hybrid design promises to be effective in achieving efficient fluid mixing [33].

METHODOLOGY

The innovative design of the static mixer

The diagram in Figure 2 shows the innovative stationary mixer design, which resembles the structure of a Tesla valve in terms of the branching of the flow streams after the liquids enter into two branches. One of them continues towards the main channel, and the other deflects towards the peripheral space that loops at its end to meet the main channel again at a repeated system. The invented cylindrical static mixer in this research was planned to have a large size with a diameter of 170 mm and a height of 600 mm. The mixer was designed to be relatively large to meet the requirements of continuous flow in water treatment plants. The dimensions of the cross sections and the longitudinal section of the repeated six-channel stages remained constant throughout the mixer. Water flowed through the main channel of the mixer while aluminium hydroxide chloride,

which was used as a coagulant, flowed into the peripheral channels. Both fluids entered the mixer at 20 °C.

To enhance the mixing performance of the employed Tesla structure mixer, the impact of two different flow pass shapes was investigated: one passing through sharp edges and the other through rounded edges. The design features and detail dimensions are shown in (Figure 3A-B) and (Figure 4). Raw water and coagulants enter the mixer from the lower openings in a flow from the bottom to the top against gravity, where the water enters directly into the main channel at a flow speed of 0.1 m/s. In comparison, the coagulated fluid enters through the peripheral channels at a flow speed of 0.3 m/s to follow the curved path and then meets at the end of this path with raw water in the main channels.

Flow solver

The computational fluid dynamics code Ansys Fluent Workbench® 2023 R2 version: 3D simulation, double resolution, pressure-based, mixture, realizable k-epsilon, transient was used to perform the simulations. The code predicts fluid mixing streams by solving partial differential equations numerically, which designate the conservation of mass and momentum. For turbulent flows, the code solved the conservation equations to obtain the average time information. The time-mean equations demonstrate the transmission of mass and momentum by turbulence.

The turbulence simulation in this study was adopted, considering the standard turbulence K-epsilon and standard wall functions with the dispersive option. The dispersive turbulence model is the appropriate model when using the granular model (ANSYS, 2023).

The grid independence test examined different mesh element sizes of 0.1 mm, 0.2 mm, 0.3 mm, and 0.5 mm using the FLUENT solver. The

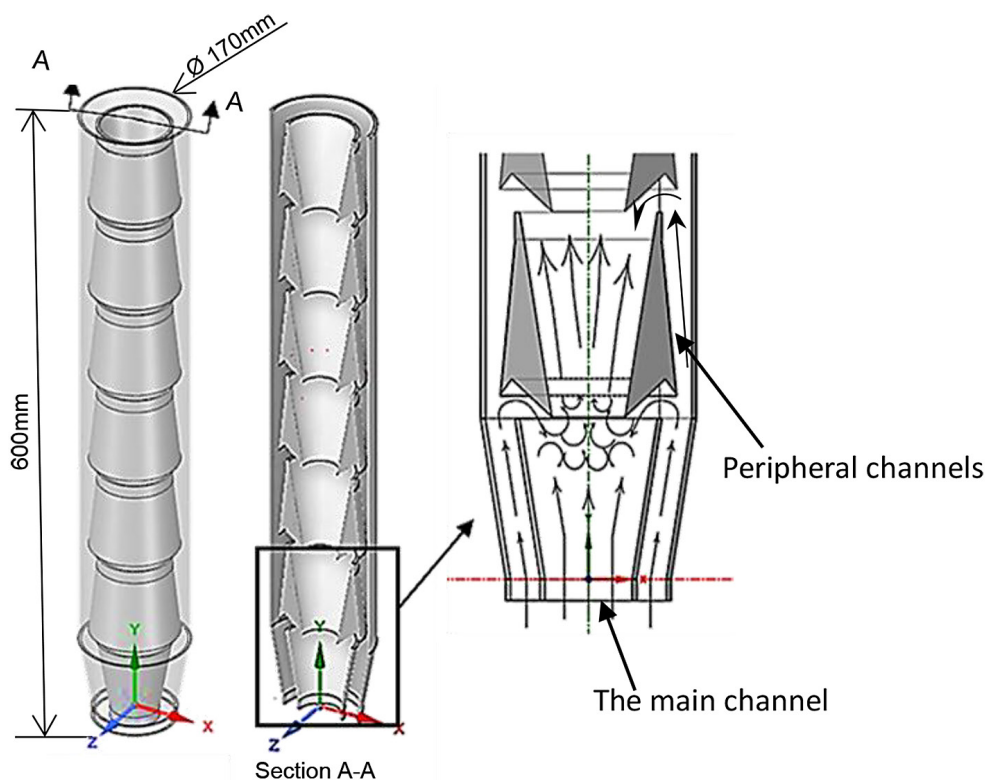


Figure 2. The innovative stationary elements' mixer design

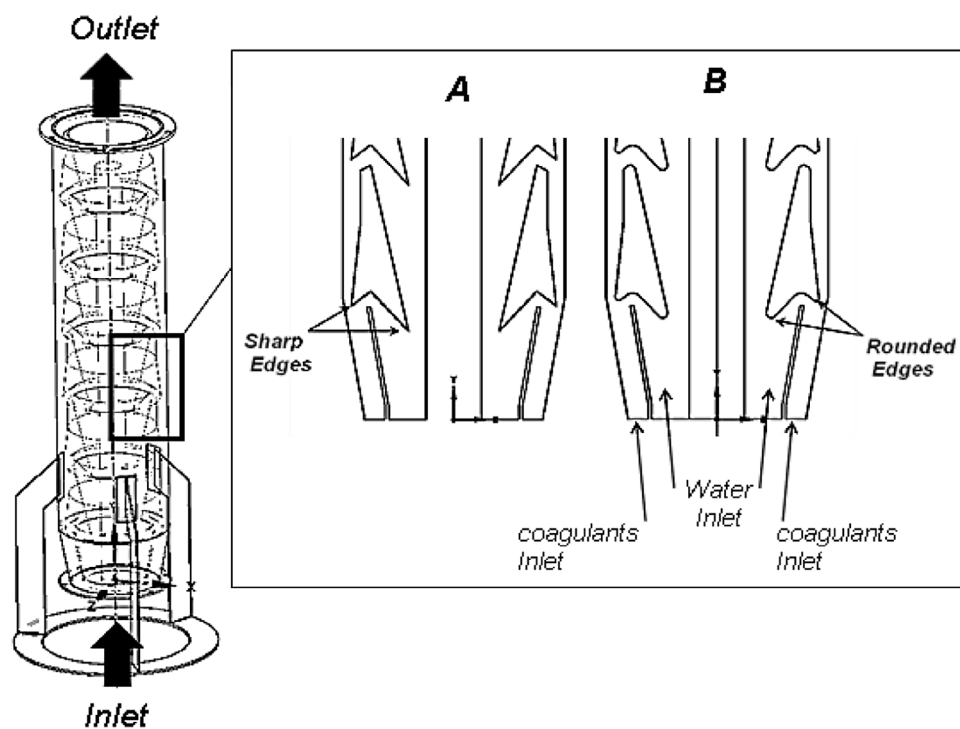


Figure 3. The two suggested designs: A) passing through sharp edges, B) passing through rounded edges

results, compared in terms of outlet pressure and velocity (see Figure 5), identified 0.3 mm as the most reliable mesh size for further analysis based on the equilibrium points close to a steady state.

For fluid phases, the simulation process was considered. Air as a primary phase, water, and aluminum hydroxide chloride as secondary phases, while the mixer walls were considered aluminum

for the proposed solid simulation. Table 1 shows the properties of the material.

DESIGN MODELING AND NUMERICAL APPROACH

Navier-Stokes equation is used for a better understanding of the mixing flow in the stationary mixer. This equation is essential in fluid mechanics and expresses the principles of mass, momentum, and energy conservation. It is commonly used to describe the behavior of Newtonian viscous fluids and can be written as follows to express the conservation of momentum:

$$(\vec{u} \cdot \nabla) \vec{u} = -\frac{\nabla p}{\rho} + \nu \nabla^2 \vec{u} \quad (1)$$

$$\nabla \cdot \vec{u} = 0 \quad (2)$$

where: \vec{u} is the velocity vector, ρ is the bulk density, p is pressure, and ν is the kinematic viscosity. Simulation of mixing continuity was embodied by solving the diffusion equation: m_d is the mass diffusivity, and m_f is the mass fraction of fluid.

$$(\vec{u} \cdot \nabla) m_f = m_d \nabla^2 m_f \quad (3)$$

Ansys® Fluent 2023 R2 was used to solve the governing Equations 1, 2, and 3 based on the finite volume method. The velocity distribution at both inlets was assumed to be uniform, and the outflow condition was applied as an outlet. The

no-slip boundary condition was specified for all inner walls were considered as a no-slip boundary.

RESULTS

Due to the symmetry of the cylindrical geometry of both mixers, an identical longitudinal plan was selected to perform the computerized fluid dynamics (CFD) of fluid behavior within the mixer channels to save time and memory in the computer. CFD analysis of mixing streams for both designs proved good mixing ratios along the mixers elevated, but it seems that the sharp-edged mixer maintained a more balanced mixing ratio for the two liquids, which meant a larger surface area for interaction between raw water and coagulants [34]. In contrast, the mixer with channels with round edges allowed the coagulant masses to flow smoothly into the main channel, occupying it almost completely at some levels. This reduced the chances of contact between raw water and coagulants. Figures 5 and 6 depict the volume of fraction (VOF) of both liquids inside both the rounded edges channel mixer and the sharp edges channel mixer sequentially and at different heights within the main channels of the mixers as an indicator of mixing ratios. During CFD analysis, different flow velocity ratios were tested for fluid inlet mixing. Both mixers showed the best mixing ratios at a water inlet flow velocity of 0.1 m/s and an inlet flow velocity of coagulant fluid of 0.3 m/s.

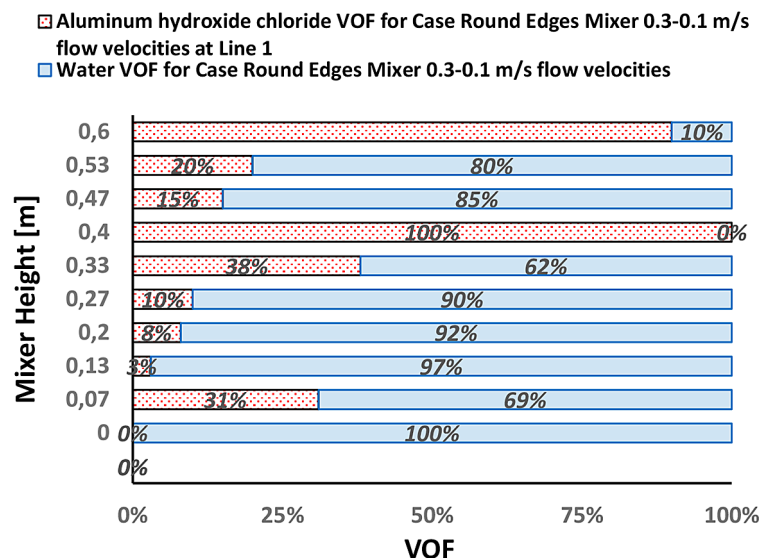


Figure 6. VOF ratios of raw water and coagulant fluid in the round edges static mixer

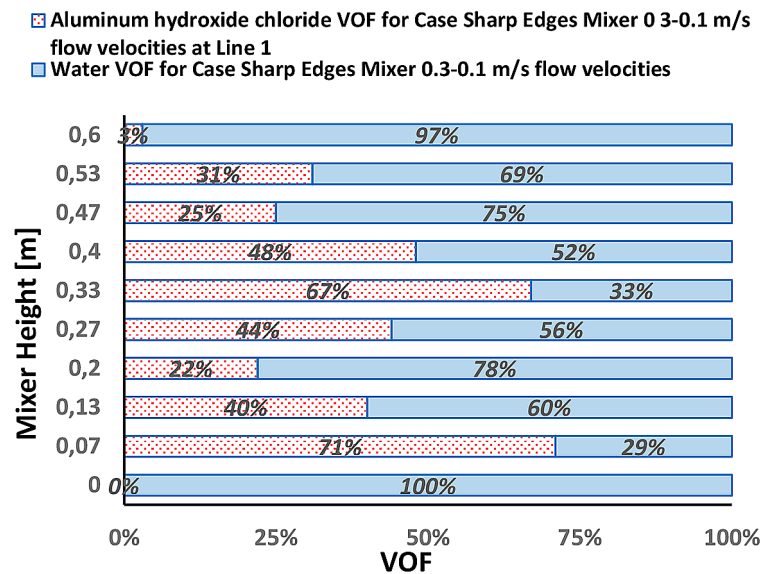


Figure 7. VOF ratios of raw water and coagulant fluid in the sharp edges static mixer

Careful observation of Figures 6 and 7 shows that the mixing ratios in the sharp edge mixer were better, as they fluctuated around 50% at most of the selected levels over the height of the mixer, while the mixing ratio was far from the ideal 50% in the round edges mixer.

The turbulent kinetic energy contour of the sharp edge mixer (Figure 8) shows a higher fluid

kinetic disturbance in the main channel than that shown in the same space in the mixer with rounded edges, indicating greater fluid mixing activity.

Figure 9A illustrates the volume of fraction (VOF) contour confirming the preference of mixing activity in the mixer with sharp edges. The presence of a balanced ratio of coagulants to the ratio of raw water flowing in the main channel,

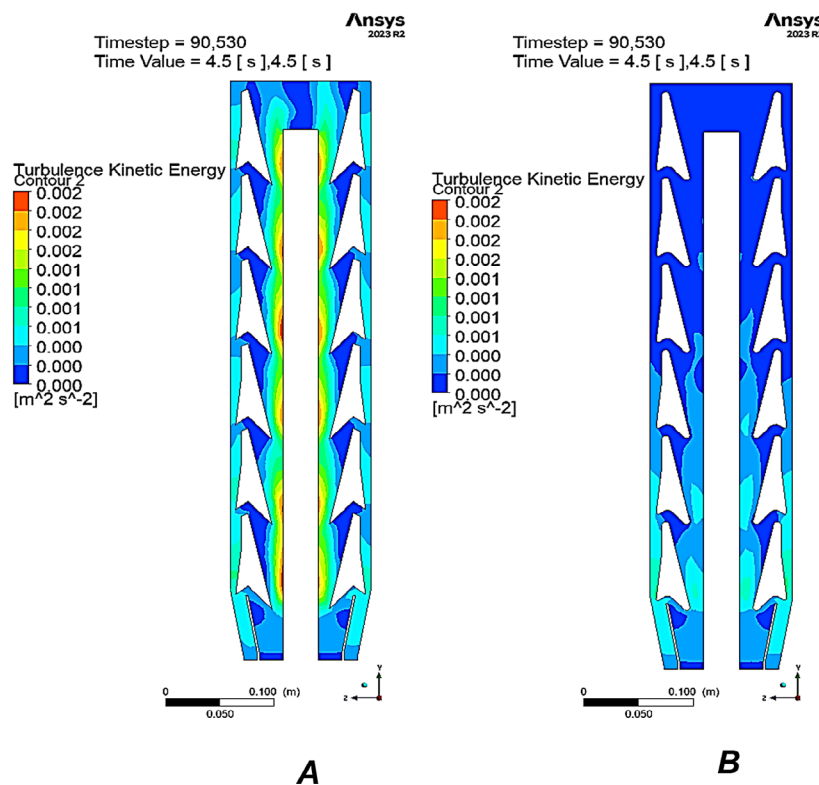


Figure 8. The turbulent kinetic energy contour for: A) sharp edge mixer, B) a rounded-edge mixer

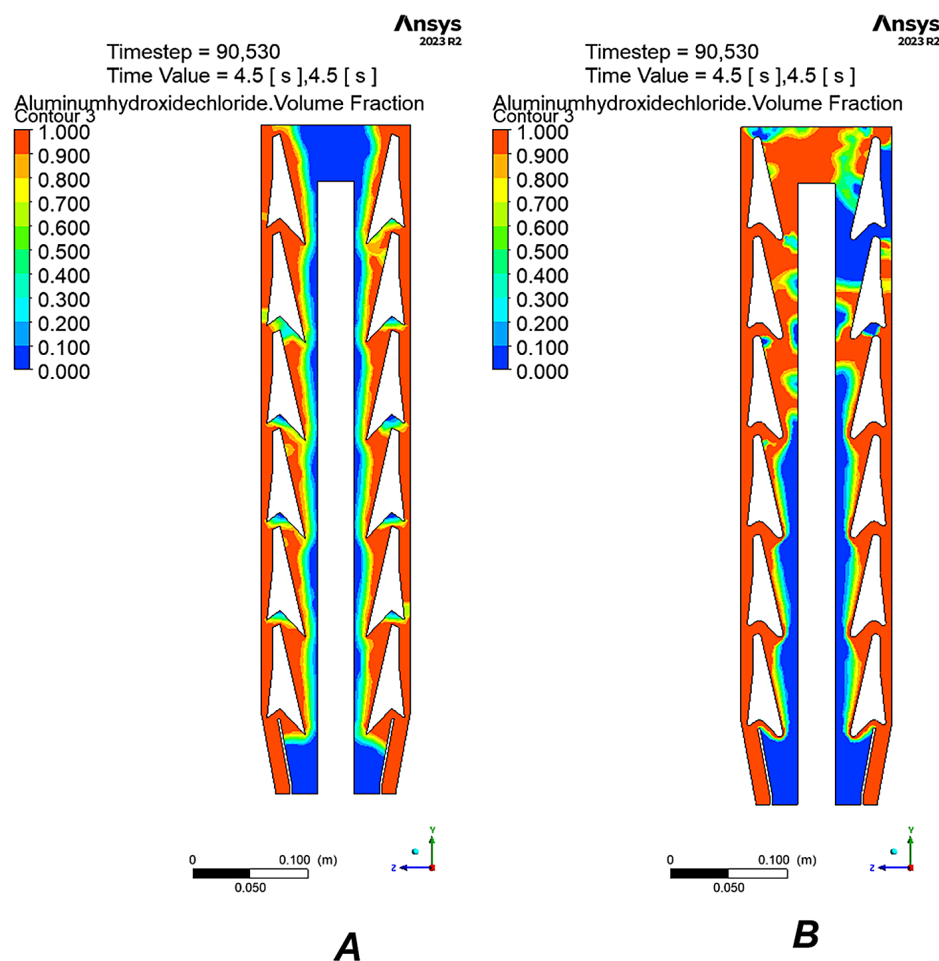


Figure 9. The VOF contour for A) sharp edge mixer, B) a rounded-edge mixer

in conjunction with the effect of stimulating kinetic energy, is represented by sufficient factors to maintain the mixing process. As it was mentioned previously, it was also observed in Figure 9B – specifically at the middle of the height of the mixer with rounded edges and above – that coagulants either occupy all the space in the main channel or are almost completely absent, which greatly reduces the chances of contact between the surfaces of the two liquids.

Design optimization

According to the analysis of the two designs, the authors proposed developing the design of the mixer with sharp edges since it has better mixing performance. Thus, the plan was to increase the number of mixing channels while maintaining the same capacity and external measurements of the mixer. This meant that the vertical trajectory measurement for each stage would be reduced. The anticipation was that the development

would increase the turbulent kinetic energy areas and mix vortices at the zones where the terminal channels converge with the main channel. The CFD analysis was performed for the modified design with identical boundary conditions, period, and time steps as the initial design.

The modified mixer showed an excellent balance in the mixing ratios between raw water and coagulation liquid. In most of the levels within the main channel of the mixer, the developed mixer achieved a mixing ratio of approximately (0.4–0.6) for the coagulation fluid and raw water, respectively. Figure 10 shows the VOF of the liquids in the mixing channels of the developed mixer.

Figure 11 compares the volume of fractions in the main channel of the mixer with sharp edges before development and the same mixer after development. Reducing the size of the coagulant fluid portion in the modified mixer provides more surface area to contact the surface of the raw water, especially when the ratio is close to a ratio of one-to-one, i.e., the value (50%) on the VOF axis

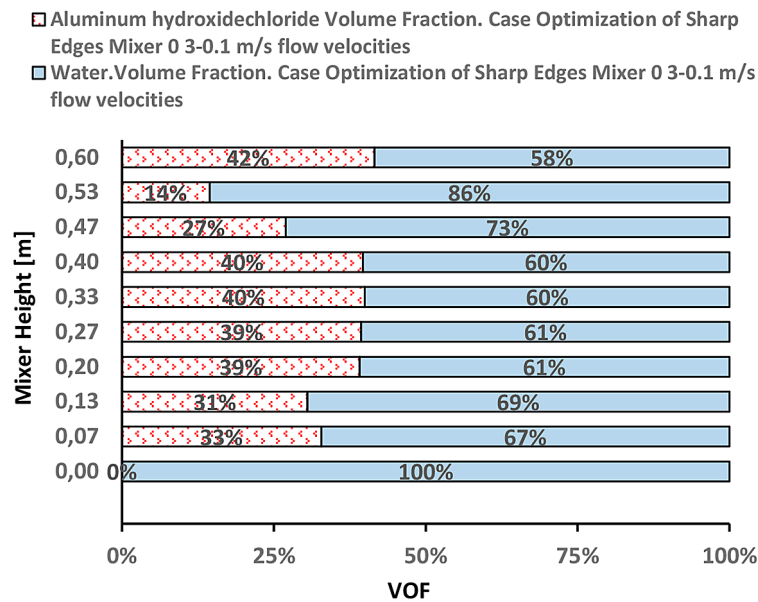


Figure 10. (VOF) Ratios of raw water and coagulant fluid for the modified sharp edges static mixer

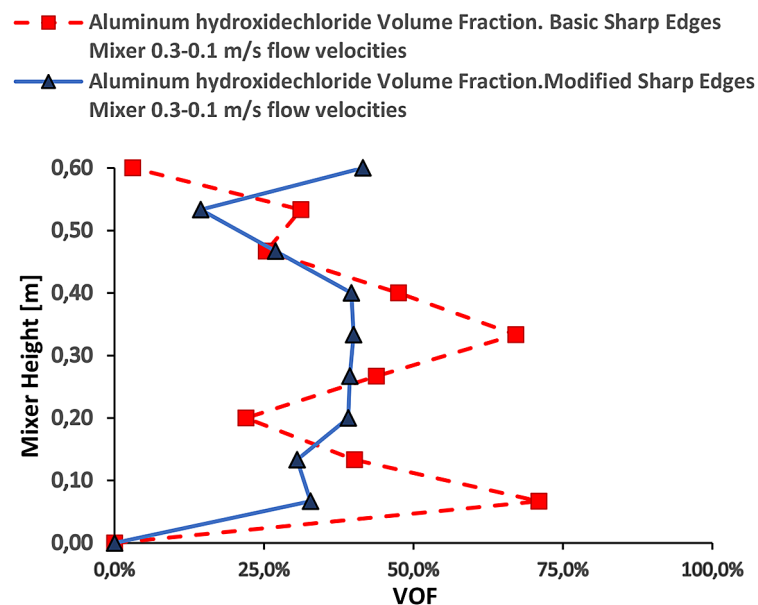


Figure 11. A comparison of the volume of fractions (VOF) in the main channel between the modified sharp edges mixer and the basic sharp edges mixer

in Figure 10, which is the ideal ratio to achieve high coagulation ratios.

Figure 12 shows the positions of the horizontal planes that were examined to display the mixing ratios. Each plane separates into two consecutive stages, and it is where the main mixing vortices occur. These levels were numbered from 1 to 8, representing the number of mixing stages for the modified mixer, which has two stages more than the basic study mixer. Level 9 represents the final pickup zone for the mixer.

Figure 13 shows the contour planes of the fraction volumes VOFs for the raw water and coagulant liquid mixture, expressing the mixing ratio. The planes are arranged in the same sequence as shown in Figure 10, where the mixing performance has progressed successively according to the mixing stages from the bottom of the mixer to its top.

The top zone of the mixer is where the mixture is collected. This zone has the largest volume and surface area in the mixer and is represented

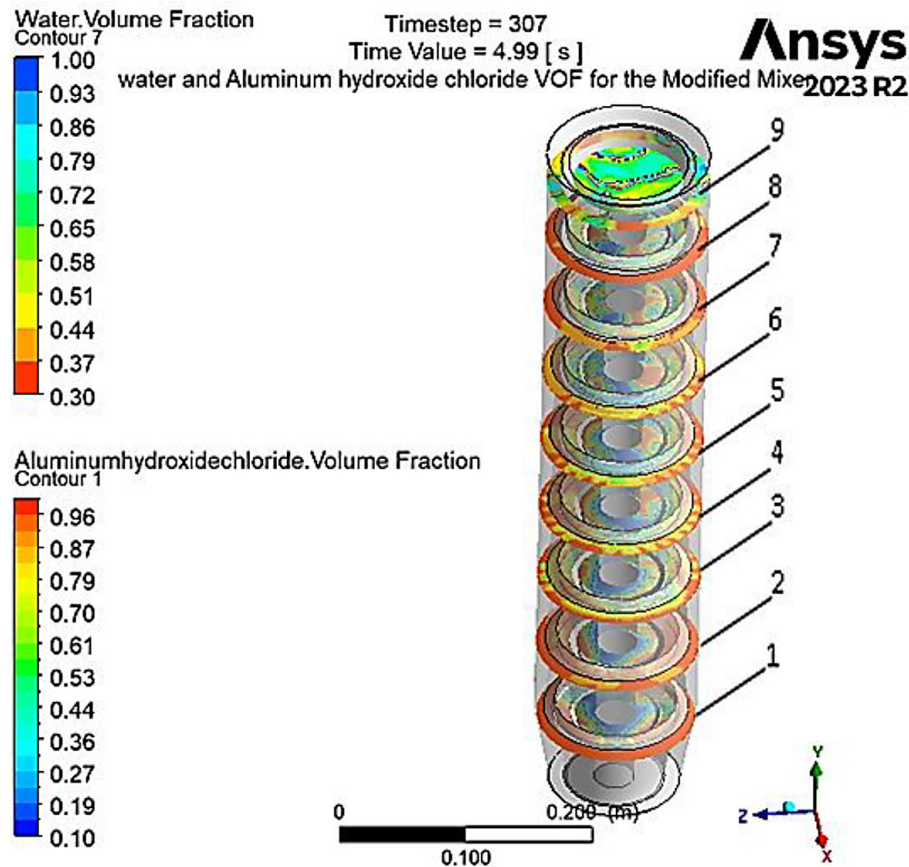


Figure 12. Positions of the VOF inspection levels for mixing fluids into the sharp edges modified mixer

by plane No. 9 in Figure 14. The contour at the top plane showed a very distinctive mixing ratio as an indicator of the high mixing efficiency of the innovative mixture.

Although the kinetic energy contour of the mixing streams within the main channel for the developed mixer indicated a lower kinetic energy (Figure 15). This did not affect the mixing performance; it seems that the stream flow dynamics that were closer to the laminar flow behavior have allowed sufficient time for the coagulants to interfere with the raw water bulk.

One of the main parameters in selecting a static mixer is the pressure drop value and mixing efficiency. Working to reduce pressure drop improves the mixing efficiency and vice versa. As the higher difference between the inlet and outlet pressure increases, the obstruction of flow in the narrow passages of the static mixer occurs, thereby delaying the mixing effectiveness.

Practically, increasing the mixing stages in the developed mixer did not make an important impact on the pressure drop compared to the basic mixer (see Figure 16), since the increase of mixer

stages was not sufficient to cause a clear effect on the pressure drop. However, the pressure drop did not exceed approximately 6 kPa in both mixers, as this drop is considered acceptable for good mixing performance.

Although the pressure drop was close in the two mixers, the modified design consistently gives slightly lower pressure drop for the same mixer height.

To quantify the percentage improvement, the following formula can be used:

$$\% \text{ Improvement} = \frac{(\Delta P_{\text{Basic}} - \Delta P_{\text{Modified}})}{\Delta P_{\text{Basic}}} \times 100\% \quad (4)$$

Thus, according to the previous improvement formula, the mixing performance of the improved sharp edge mixer was compared to the basic design of the sharp edge mixer through the use of the pressure difference depreciation index, where the percentage of improvement was obtained equal to 16%.

The modified mixer with eight stages utilized the Tesla mixer flow principle, resulting in an

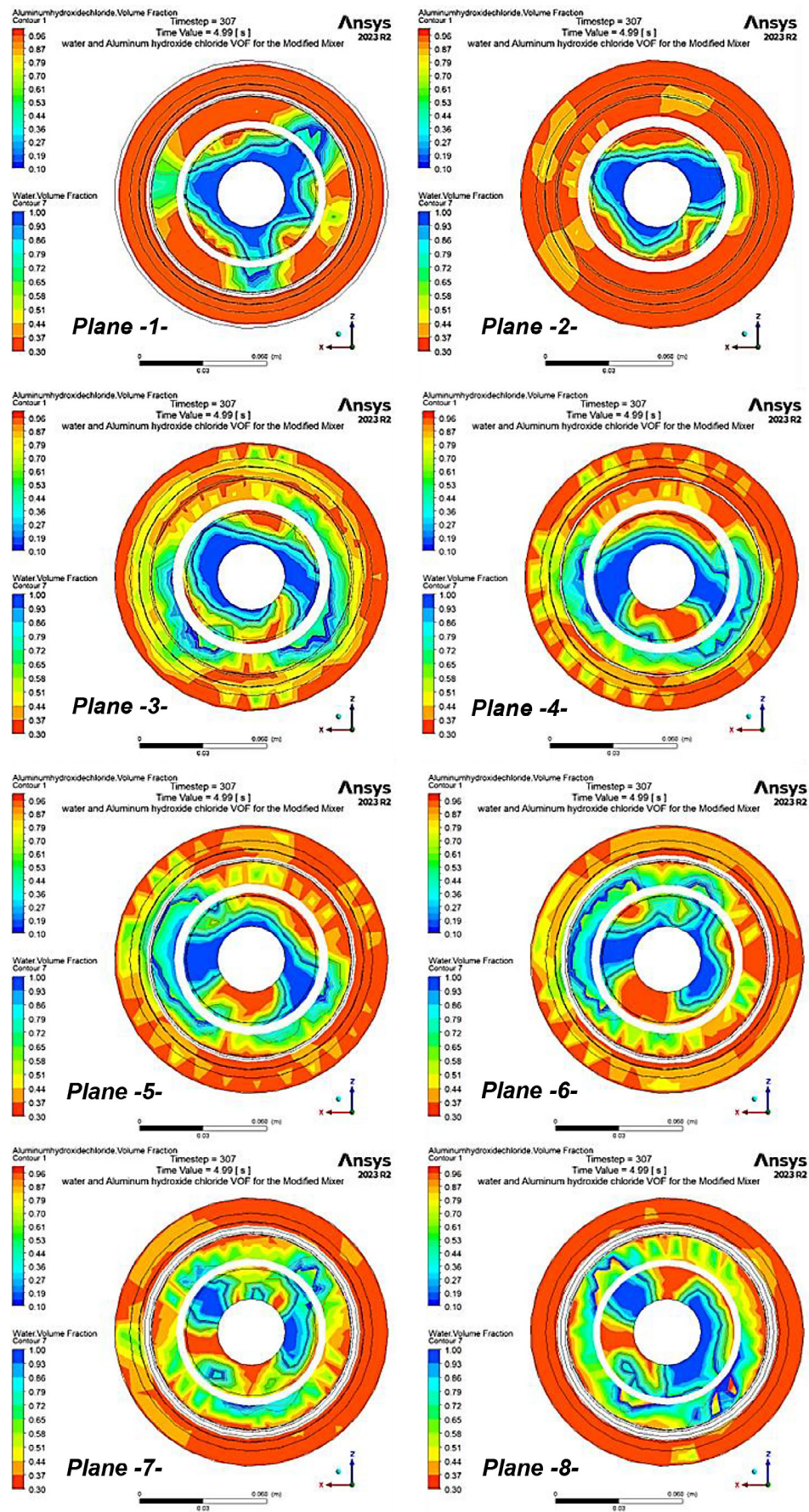


Figure 13. The contour of the volumes of fraction (VOFs) for the raw water and coagulant liquid mixture in the modified mixer

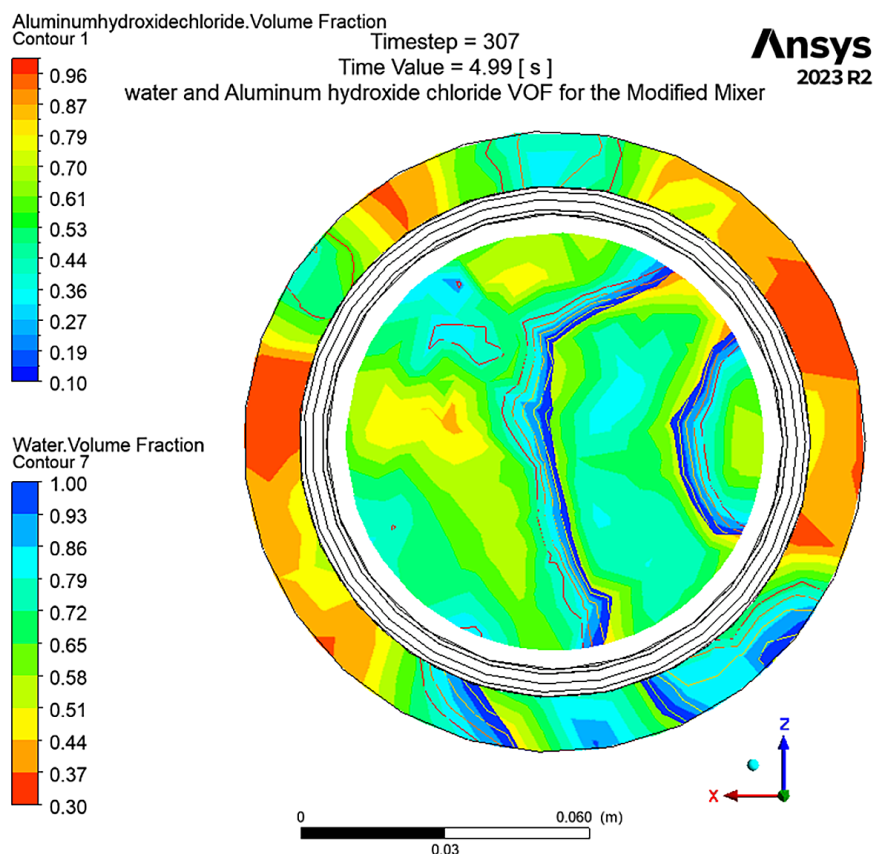


Figure 14. Plane No. 9 contour of the volume of fraction (VOF) for the raw water and coagulant liquid mixture

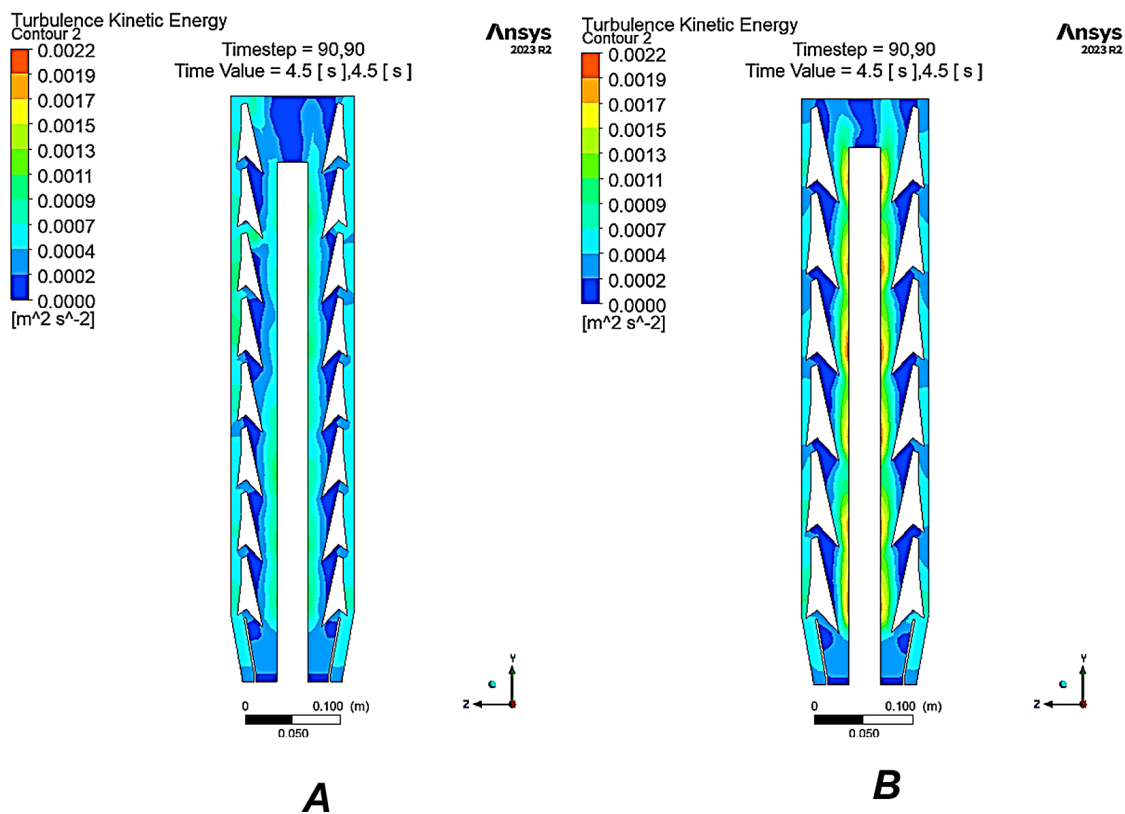


Figure 15. A comparison of the kinetic energy contour for the: A) modified sharp edges mixer, B) basic sharp edges mixer

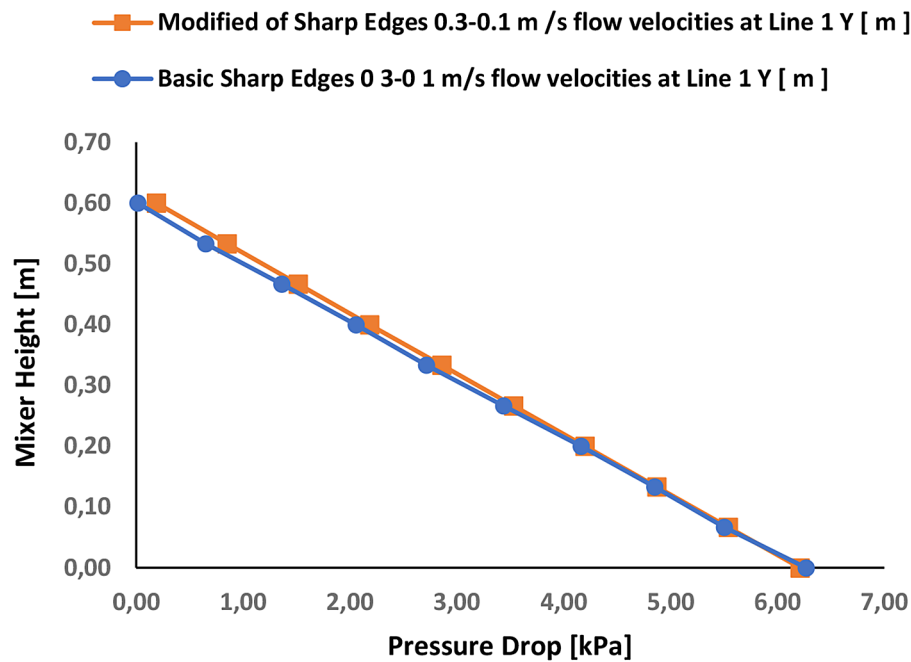


Figure 16. Pressure drop comparison between the basic and the modified sharp-edged mixer

optimal mixing ratio. Its innovative engineering design was simple, which contributed to its success through maintaining a distinct flow momentum while reducing pressure drops at its lowest levels.

CONCLUSIONS

This research aimed to create an innovative, large-sized, low-complexity static mixer with fixed mixing elements that maintain minimal pressure drop while conserving kinetic energy in the mixing tracks. The new design adopted the concept of the Tesla micromixer structure modified for the mixing task in water treatment applications. Two new static mixer designs were tested using CFD analysis. The first design had flow channels with sharp edges, while the second design had the same channels but with rounded edges. The analysis of the mixers was carried out under the same operational boundary conditions and for the same period.

The CFD analysis revealed that the mixer with sharp channel edges had improved mixing performance in terms of better mixing ratios, less pressure drop, higher flow momentum, and intense kinetic energy. Optimal mixing performance was achieved in the sharp-edged channels mixer by further modification through increasing the number of mixing stages while maintaining the same size of the mixer. This improvement

was accomplished for two main reasons: First, the mixer design was altered to enhance the interaction between coagulants from the peripheral channels and the raw material in the main channel, thereby increasing the number of mixing vortices in those areas. Second, these vortex zones themselves contributed to maintaining the velocity and momentum of the flow towards the flow of the mixing streams under the condition of a pressure drop by an acceptable percentage.

Acknowledgment

The authors gratefully acknowledge the support of Middle Technical University and Al-Naji University, which sponsored this research as part of its commitment to advancing scientific knowledge and fostering academic excellence

REFERENCES

1. Al-Amshawee S.K.A., Yunus M.Y.B.M., Alalwan H.A., Lee W.H., Dai F., Experimental investigation of biofilm carriers of varying shapes, sizes, and materials for wastewater treatment in fixed bed biofilm reactor: a qualitative study of biocarrier performance, *Journal of Chemical Technology & Biotechnology*, 2022; 97: 2592–2606.
2. Hassan M.M., Abudi Z.N., Al-Furaiji M.H., Farsani R.Y., Removal of Congo red dye using

- polyvinylidene fluoride polymer in application ultrafiltration membranes, *Journal of Engineering and Sustainable Development*, 2025; 29: 532–538.
3. Alalwan H.A., Alminshid A., Mohammed M.M., Mohammed M.F., Spectroscopic investigation of carbon dioxide interactions with transition metal-oxide nanoparticles, *Chemical Engineering & Technology*, 2023; 46: 587–594.
4. Alalwan H.A., Alminshid A.H., Mohammad M., Hussein S.A.M., Mohammed M.F., Employing synthesized MgO-SiO₂ nanoparticles as catalysts in ethanol conversion to 1, 3-Butadiene, *International Journal of Nanoscience and Nanotechnology*, 2022; 18: 157–166.
5. Alalwan H.A., Alminshid A. H., Mohammed M.M., Mohammed M.F., Methane activation on metal oxide nanoparticles: spectroscopic identification of reaction mechanism, *Particulate Science and Technology*, 2022; 1–8.
6. Hassan Q.H., Ali N.S.M., Alalwan H.A., Alminshid A.H., Mohammed M.M., The impact of adding nanoparticles to biodiesel fuel prepared from waste sunflower oil on the performance and emission of diesel engines, *Circular Economy*, 2025; 4: 100138.
7. Alminshid A.H., Alalwan H.A., Mohammed M.M., Abbas M.N., Spectroscopic study of methane reaction mechanism on MgO nanoparticles, *Ionics*, 2025; 1–6.
8. Shadhar M.H., Salih B.M.M., Khaleel O.R., Kadhim Y.M., Mohammed M.M., Alalwan H.A., The influence of eggshell nanoparticles as a partial replacement of cement in concrete, *Innovative Infrastructure Solutions*, 2024; 9: 465.
9. Saritha V., Namuduri S., Vuppala S., NV, Analysis and optimization of coagulation and flocculation process, *Applied Water Science*, 2017; 7: 451–460.
10. Ohm T.I.a.C., Seong J., Zhang, Yu M., and Joo, Chul J., Computational fluid dynamics modeling and field applications of non-powered hydraulic mixing in water treatment plants, *Water*, 2020; 12.
11. Habl A., Amooey A., Mustafa M., Alalwan H.A., Electro oxidation process for wastewater treatment in petroleum refineries, *Pollution*, 2024; 10: 819–832.
12. Al-Furaiji M., Kadhom M., Waisi B., Kalash K., Coupled effect of organic fouling and scaling in the treatment of hyper-saline produced water using forward osmosis, 2023; 210.
13. Alalwan H.A., Ali N.S.M., Mohammed M.M., Mohammed M.F., Alminshid A.H., A comparison study of methyl green removal by peroxi-coagulation and peroxi-electrocoagulation processes, *Cleaner Engineering and Technology*, 2023; 13: 100623.
14. Waseem M., Omar I., Jawad M., Saidani T., Al-Mdallal Q.M., Impact of Cattaneo-Christov heat and surface temperature on viscoelastic non-newtonian micropolar nanofluids: Darcy exponential sheet flow with planktonic microorganisms, *International Journal of Thermofluids*, 2025; 26.
15. Kalash K.R., Al-Furaiji M.H., Waisi B., Ali R.A., Evaluation of adsorption performance of phenol using non-calcined Mobil composition of matter no. 41 particles, *Desalin. Water Treat.*, 2020; 198: 232–240.
16. Qiao Y., Longyun Z., and Kai G., Hui L., Bao Z., Wei L., Xiang G., Chunjiang L., Numerical study of flow field and mixing performance of a new curved-sheet blade-folded static mixer, *Industrial & Engineering Chemistry Research*, ACS Publications, 2024; 7836–7852.
17. Rahmani R.K.K., Theo G. and Anahita A., Numerical simulation of turbulent flow in an industrial helical static mixer, *International Journal of Numerical Methods for Heat & Fluid Flo*, Emerald Group Publishing Limited, 2008; 675–696.
18. Banerjee A., Mazumdar J., A numerical investigation on rheological turbulent flow through a 90° mixing elbow, *Journal of Engineering and Applied Science*, 2024; 71: 209.
19. Zalc J.M., Szalai E.S., Muzzio F.J., Jaffer S., Characterization of flow and mixing in an SMX static mixer, *AIChE Journal*, 2002; 48: 427–436.
20. Tariq S.M., Asim M., Ahmed U., Ahmed Q.R., Uddin A.Z., Muhammad H., Uzair A., Sarfaraz A.S., Mariyam, S., Numerical Simulation of Low-Pressure Drop Static Mixers for Mixing Enhancement}, 2022; 41.
21. [Soman S.S.M., Chandra M.R, Effects of internal geometry modifications on the dispersive and distributive mixing in static mixers, *Chemical Engineering and Processing: Process Intensification*, Elsevier, 2017; 31–43.
22. Mathew V., Smart D.S.R., Wins K.L.D., Dhas D.S.E.J., Effect of temperature, geometric parameters, and surface conditions on fluid mixing in a vertical port static mixer, *Engineering Research Express*, IOP Publishing, 2024; 015022.
23. Zhao S., Runze H., Nie Y., Lianzhu S., Wei H., Ning Z., Yuguang L., Dong J., Kai G., Intensification of mixing efficiency and reduction of pressure drop in a millimeter scale T-junction mixer optimized by an elliptical array hole structure, *Chemical Engineering and Processing-Process Intensification*, Elsevier, 2022; 109034.
24. Al-Furaiji M., Waisi B., Kalash K., Kadhom M., Effect of polymer substrate on the performance of thin-film composite nanofiltration membranes, 2022; 27.
25. Nyande B.W., Kiran M.T., Lakerveld R., CFD analysis of a Kenics static mixer with a low pressure drop under laminar flow conditions, *Industrial & Engineering Chemistry Research*}, ACS Publications, 2021; 5264–5277.

26. Al-Mousawi F.N., Dhaidan N.S., Homod R.Z., Al-Dadah R., Mahmoud S., Al Jubori A.M., Daabo A.M., Chalok K.H., An efficient small-scale radial inflow turbine for an adsorption system for cooling and electricity: A comprehensive CFD analysis, *International Communications in Heat and Mass Transfer*, 2025; 162.
27. Bahlekeh A., Mohammed H.I., Al-Azzawi W.K., Dulaimi A., Majdi H.S., Talebizadehsardari P., Mahdi J.M., CFD analysis on optimizing the annular fin parameters toward an improved storage response in a triple-tube containment system, *Energy Science and Engineering*, 2022; 10: 4814–4839.
28. Tesla N., Valvular conduit. In: U.S.P.a.t. Office. (Ed.) USA, 1920.
29. Ben M.B., Hamida, Mohsen A.M., Hussein M.A., Rajab H., Chamkha A., A CFD based optimization procedure of operating parameters for an impinging jet on moving fabric subject to thermal dipping process, *International Communications in Heat and Mass Transfer*, 2025; 167.
30. Al-Rbeawi S., Pressure distributions and flow regimes: An integrated approach for CO₂ sequestration project design and evaluation in hydraulically fractured shale reservoirs, *Gas Science and Engineering*, 2025; 133.
31. Hong C.C., Choi J.W., Ahn C.H., A novel in-plane passive microfluidic mixer with modified Tesla structures, *Lab on a chip*, 2004; 4: 109–113.
32. Wang J., Cong X., Mini liquid-liquid extractor without moving parts based on the Coanda effect, *Chemical Engineering & Technology*, 2014; 37: 535–542.
33. Al-Furaiji M.H.O., Karim U.F.A., Augustijn D.C.M., Waisi B.I.H., Hulscher S.J.M.H., Evaluation of water demand and supply in the south of Iraq, *Journal of water reuse and desalination*, 2016; 6: 214–226.
34. Alsehli M., Basem A., Jasim D.J., Mausam K., Alshamrani A., Sultan A.J., Kassim M., Rajab H., Musa V.A., Maleki H., Insights into water-lubricated transport of heavy and extra-heavy oils: Application of CFD, RSM, and metaheuristic optimized machine learning models, *Fuel*, 2024; 374.